



# The characterization of structure, thermal stability and magnetic properties of Fe–Co–B–Si–Nb bulk amorphous and nanocrystalline alloys

S. Lesz<sup>a</sup>, R. Babilas<sup>a</sup>, M. Nabiałek<sup>b,\*</sup>, M. Szota<sup>b</sup>, M. Dośpiał<sup>b</sup>, R. Nowosielski<sup>a</sup>

<sup>a</sup> Institute of Engineering Materials and Biomaterials, Silesian University of Technology, Gliwice, Poland

<sup>b</sup> Czestochowa University of Technology, Czestochowa, Poland

## ARTICLE INFO

### Article history:

Received 5 August 2010

Received in revised form

14 December 2010

Accepted 17 December 2010

Available online 31 December 2010

### Keywords:

Amorphous materials

Ferromagnetic materials

Magnetic hysteresis

X-ray measurements

## ABSTRACT

Recently bulk amorphous alloys have attracted great attention due to their excellent magnetic properties. The glass-forming ability of bulk amorphous alloys depends on the temperature difference ( $\Delta T_x$ ) between glass transition temperature ( $T_g$ ) and crystallization temperature ( $T_x$ ). The increase of  $\Delta T_x$  causes a decrease of the critical cooling rate ( $V_c$ ) and growth of the maximum casting thickness of bulk amorphous alloys. The aim of the present paper is to characterize the structure, the thermal stability and magnetic properties of Fe<sub>36</sub>Co<sub>36</sub>B<sub>19</sub>Si<sub>5</sub>Nb<sub>4</sub> bulk amorphous alloys using XRD, Mössbauer spectroscopy, DSC and VSM methods. Additionally the magnetic permeability  $\mu_i$  (at force  $H \approx 0.5$  A/m and frequency  $f \approx 1$  kHz) and the intensity of disaccommodation of magnetic permeability  $\Delta\mu/\mu(t_1)$  ( $\Delta\mu = \mu(t_1 = 30 \text{ s}) - \mu(t_2 = 1800 \text{ s})$ ), have been measured, where  $\mu$  is the initial magnetic permeability measured at time  $t$  after demagnetisation, the Curie temperature  $T_c$  and coercive force  $H_c$  of rods are also determined with the use of a magnetic balance and coercivemeter, respectively.

Fe–Co–B–Si–Nb bulk amorphous alloys were produced by pressure die casting with the maximum diameters of 1 mm, 2 mm and 3 mm.

The glass transition temperature ( $T_g$ ) of studied amorphous alloys increases from 807 K for a rod with a diameter of 1 mm to 811 K concerning a sample with a diameter of 3 mm. The crystallization temperature ( $T_x$ ) has the value of 838 K and 839 K for rods with the diameters of 1 mm and 3 mm, respectively. The supercooled liquid region ( $\Delta T_x = T_x - T_g$ ) has the value of about 30 K. These values are presumed to be the origin for the achievement of a good glass-forming ability of the Fe–Co–B–Si–Nb bulk amorphous alloy. The investigated amorphous alloys in the form of rods have good soft magnetic properties (e.g.  $M_s = 1.18$ – $1.24$  T). The changes of crystallization temperatures and magnetic properties as a function of the diameter of the rods (time of solidification) have been stated.

© 2010 Elsevier B.V. All rights reserved.

## 1. Introduction

The first Fe-based bulk metallic glasses (BMGs) were prepared in 1995 [1], since then, iron-based bulk metallic glasses have been studied as a novel class of engineering materials, which have a good glass forming ability and soft magnetic properties [1–6]. For example, in 2004, Inoue et al. synthesized [(Fe<sub>x</sub>Co<sub>1-x</sub>)<sub>0.75</sub>B<sub>0.2</sub>Si<sub>0.05</sub>]<sub>96</sub>Nb<sub>4</sub> ( $x = 0.1$  and  $-0.5$  at.%). BMGs exhibit good soft magnetic properties, as well as superhigh fracture strength of 3000–4000 MPa and ductile strain of 0.002 [4]. Researching a Fe-based BMGs with high GFA and excellent magnetic and mechanical properties, the effect of the replacement of Fe by Co and alloying addition has been investigated.

Newly developed Fe- and Co-based bulk metallic glasses are attractive compared with conventional crystalline alloys and are very useful in a wide range of engineering applications and their application fields have a tendency to be extended widely. They are suitable materials for many electrical devices such as electronic measuring and surveillance systems, magnetic wires, sensors, band-pass filters, magnetic shielding, precision mold material, precision imprint material, and cutting tool material [2,7,8].

In the present paper structure, the thermal stability and magnetic properties of Fe–Co–B–Si–Nb bulk amorphous alloys have been characterized.

## 2. Experimental

Investigations were carried out on amorphous and partially crystallized rods with the compositions of Fe<sub>36</sub>Co<sub>36</sub>B<sub>19</sub>Si<sub>5</sub>Nb<sub>4</sub>. Fe-based master alloy ingots with the above compositions were prepared by induction melting of mixtures of pure Fe, Co and Nb metals and pure B and Si crystals in an argon atmosphere. The alloy compositions represent nominal atomic percentages.

\* Corresponding author at: Czestochowa University of Technology, Institute of Physics, Armii Krajowej Av. 19, 42 200 Czestochowa, Ślaskie, Poland.  
Fax: +48 34 3250795.

E-mail address: [nmarcell@wp.pl](mailto:nmarcell@wp.pl) (M. Nabiałek).

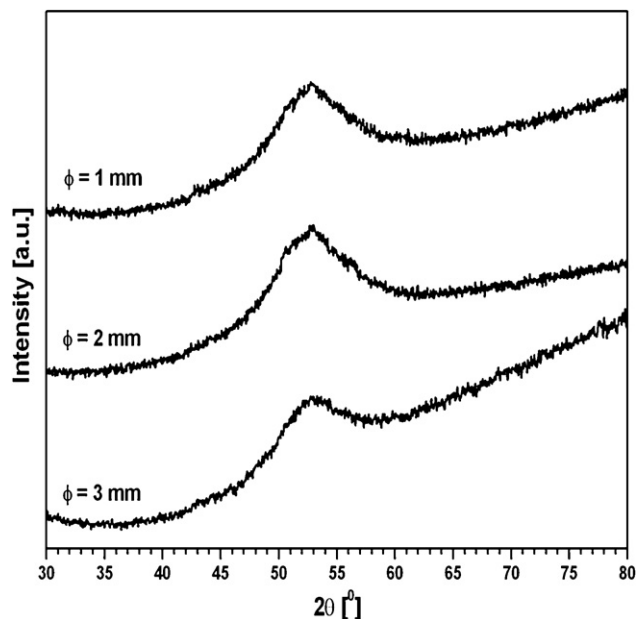


**Fig. 1.** X-ray diffraction pattern of the bulk  $\text{Fe}_{36}\text{Co}_{36}\text{B}_{19}\text{Si}_5\text{Nb}_4$  alloys in the form of rods with various diameter.

$\text{Fe-Co-B-Si-Nb}$  bulk alloys were produced by pressure die casting as presented in [9] with the diameters of 1 mm, 2 mm and 3 mm.

Structure analysis of the studied material was carried out using an X-ray diffraction (XRD) and Mössbauer spectroscopy. Seifert-FPM XRD 7 diffractometer with  $\text{Co-K}\alpha$  radiation, used for the examination of rod samples. The transmission Mössbauer spectra were recorded using a conventional POLON spectrometer with constant-acceleration and the  $^{57}\text{Co}$  of  $\gamma$ -ray source in a rhodium matrix with intensity of 50 mCi and half-life time of 273 days.

The thermal properties associated with crystallization temperature of the amorphous and partially crystallized rods were measured using the differential scanning calorimetry (DSC, Setaram). The supercooled liquid region ( $\Delta T_x = T_g - T_x$ ), of the investigated alloys was also calculated. The Curie temperature of the investigated glassy rods was determined by measuring the volume of magnetization as a function of temperature. The Curie temperature of amorphous phase was calculated from the condition  $dM(T)/dT = \text{minimum}$  [10]. The initial magnetic permeability was measured by using the Maxwell–Wien bridge. The applied magnetic field had the value of 0.5 A/m and frequency of about 1 kHz. The magnetic after effects ( $\Delta\mu/\mu$ ) were determined by measuring the changes of magnetic permeability of the examined alloys as a function of time after demagnetization, where  $\Delta\mu$  is the difference between magnetic permeability determined at  $t_1 = 30$  s and  $t_2 = 1800$  after demagnetization and  $\mu$  at  $t_1$  [11–16]. High field magnetization curves were measured by a vibrating sample magnetometer (VSM) in a magnetic field up to 2 T. The magnetizing field was parallel to the sample length to minimize demagnetization effect. The magnetization curves were analyzed using the least squares method.

The coercive force  $H_c$  of the rods was investigated with the use of a coercivemeter with a permalloy probe.

### 3. Results and discussion

It was found from the obtained results of structural studies performed by X-ray diffraction that in as quenched state the structure of the rods of  $\text{Fe}_{36}\text{Co}_{36}\text{B}_{19}\text{Si}_5\text{Nb}_4$  alloy consists of an amorphous phase, which is seen on the diffraction pattern in the form of a single broad maximum originating from the amorphous phase (Fig. 1).

The accuracy of X-ray diffractometer is about 3%. Much more sensitive is Mössbauer spectrometer and provides information from the entire volume of the sample. Therefore analysis of the Mössbauer spectra were used to confirm the amorphous structure of the samples on the basis of previously performed X-ray diffraction measurements. Fig. 2 presents Mössbauer spectra for all investigated samples.

The spectrum observed for sample presented in Fig. 2a was consisted of wide, symmetric and overlapping lines typical for amorphous ferromagnets. The amorphous structure in

**Table 1**

$(B_{\text{eff}})_{\text{I am}}$  and  $(B_{\text{eff}})_{\text{II am}}$ , the average hyperfine induction of magnetic field and FWHM of its distribution  $\sigma_{\text{I am}}$  and  $\sigma_{\text{II am}}$  for first and second amorphous phase, respectively. Relative contribution of second amorphous phase,  $X_{\text{am}}$  and crystalline phase,  $X_{\text{cr}}$  in the field distribution.

Phase	Parameter	Ø 1 mm	Ø 2 mm	Ø 3 mm
I amorphous	$(B_{\text{eff}})_{\text{I am}}$ [T]	21.1	20.1	20.8
	$\sigma_{\text{I am}}$ [T]	5.24	5.35	5.41
II amorphous	$(B_{\text{eff}})_{\text{II am}}$ [T]		29.7	
	$\sigma_{\text{II am}}$ [T]		2.36	
	$X_{\text{am}}$ [%]		10	
Crystalline	$B_{\text{cr}}$ [T]			33.2
	$\sigma_{\text{cr}}$ [T]			1.2
	$X_{\text{cr}}$ [%]			5

$\text{Fe}_{36}\text{Co}_{36}\text{B}_{19}\text{Si}_5\text{Nb}_4$  samples in the form of rods with the diameters of 2 and 3 mm was not confirmed.

For sample in the form of rod with a diameter of 2 mm (Fig. 2c), it was possible to fit to the Mössbauer spectrum, an additional Zemman sextet, characterized by relatively broad lines, that testifies about the existence of second amorphous phase in which the crystalline nuclei are already present or soon it will come to their creation. For the transmission Mössbauer spectrum obtained for sample with the highest diameter (Fig. 2e) except the presence of wide, diffused sextet corresponding to the amorphous phase was possible to fit a narrow Zemman sextet indicating existence of crystalline phase, which in based on Frąckowiak et al. [17] was identified as  $\alpha$ -FeCo.

The hyperfine fields distributions obtained from the Mössbauer spectra shows that in the main amorphous matrix the areas with different iron concentrations can be distinguished, which in turn may suggest the presence of low and high field components. On the hyperfine fields distributions obtained for rod with a diameter of 2 mm is possible to observe the second component, presumably originating from the second amorphous phase, this can be inferred from a large half-width of the decomposition of  $\sigma = 2.36$  T. For sample with the largest diameter presence of extra component in hyperfine fields distribution, due to a narrow half-width of the decomposition, can be linked to the presence of newly emerging crystalline  $\alpha$ -FeCo phase. Data obtained from the analysis of Mössbauer spectra are given in Table 1.

According to studies presented in the works [8,18] in the Co–B and Fe–B metal – metalloid type of alloys a unique network-like atomic configuration can be observed. In this type of configuration distorted trigonal prisms of Fe or Co and B are connected with each other in edge and face-shared configuration modes through “glue” atoms like Ln, Zr, Hf, Nb or Ta. This network-like short range ordering (SRO) atomic configuration can affect the rearrangement of atoms in the alloy during the diffusion processes that lead to temporary stabilization of liquid state (SL). The existence of the described SRO arrangement in all bulk amorphous alloys based on Co and Fe with the transition metals and metalloids addition, leads to presence of a primary crystallization phase with fcc complex  $(\text{Fe,Co})_{23}\text{B}_6$ , a large lattice parameter of about 1.2 nm and including 96 atoms in a volume unit.

On the basis of the Mössbauer measurements the presence of  $(\text{Fe, Co})_{23}\text{B}_6$  crystalline phase in all investigated samples could not be confirmed. In addition, grains of  $\alpha$ -FeCo phase present in the amorphous matrix are very small what can be concluded from the fact that clear, narrow peaks showing the presence of crystalline phase do not appear on the X-ray diffraction patterns. Only the use of Mössbauer spectroscopy allow to disclose the presence of  $\alpha$ -FeCo crystalline phase in sample in the form of rod with the highest diameter.

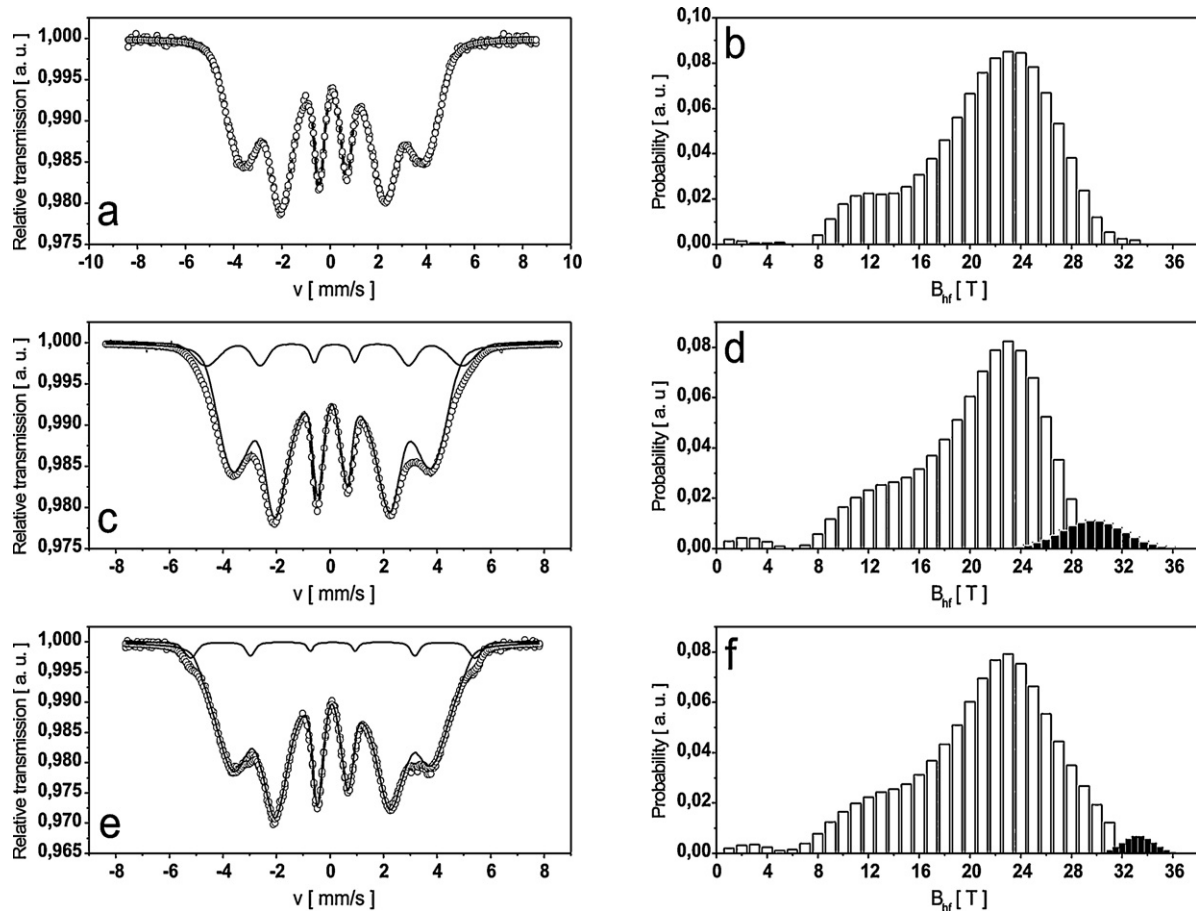


Fig. 2. Transmission Mössbauer spectra (a, c, and e) and corresponding hyperfine field distributions (b, d, and f) of the  $\text{Fe}_{36}\text{Co}_{36}\text{B}_{19}\text{Si}_5\text{Nb}_4$  alloy in the as-quenched state measured for samples in the form of rods with 1 mm, 2 mm and 3 mm diameter, respectively.

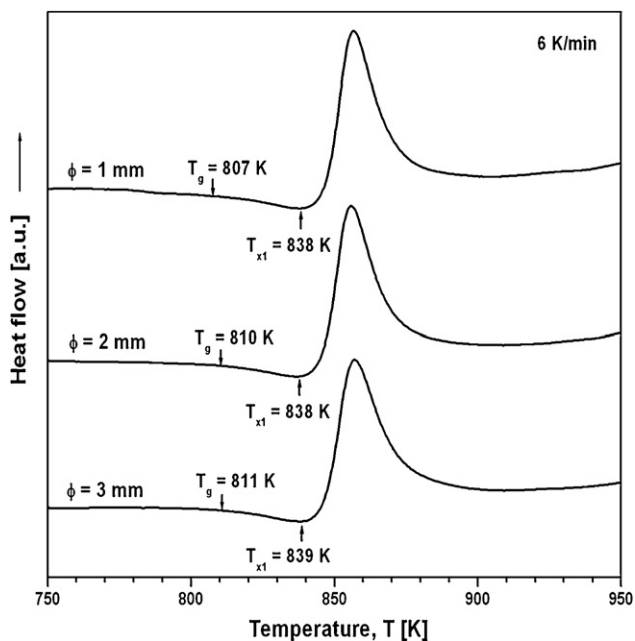


Fig. 3. DSC curves of  $\text{Fe}_{36}\text{Co}_{36}\text{B}_{19}\text{Si}_5\text{Nb}_4$  glassy and partially crystallized alloy rods with the diameters of 1 mm, 2 mm and 3 mm.

The DSC curve determined rod with a diameter of 1 mm, 2 mm and 3 mm in as-cast state for the studied alloy is shown in Fig. 3, Table 2. Glass transition temperature –  $T_g$ , onset crystallization temperature –  $T_{x1}$  and supercooled liquid region –  $\Delta T_x$  for glassy rod samples with the diameters of 1–3 mm are in the range of 807–811 K, 838–839 K and 31–28 K, respectively. The value of the supercooled liquid region is an experimental parameter that determines the glass forming ability of the tested alloy.

Comparing these results with those obtained by Stoica et al. [18] for samples in the form of rods with various diameter and a very similar composition it can be assumed that in the amorphous matrix a specific clusters or even crystalline nuclei, defined as the SRO [8] which need a large activation energy to start the crystallization process are present. Stoica et al. [18] defined an exponent in Avrami equation, which was equal to 1.43 and was close to the value of 1.5, what indicates, according to Wunderlich et al. [19], that in this kind of bulk amorphous alloys occurs SRO-type arrangement, which plays a central role in the crystallization process.

Table 2  
Thermal properties of the bulk amorphous and partially crystallized  $\text{Fe}_{36}\text{Co}_{36}\text{B}_{19}\text{Si}_5\text{Nb}_4$  rods.

Diameter, mm	Thermal properties ( $T_g$ ), K	$T_{x1}$ , K	$\Delta T_x$ , K
1	807	838	31
2	810	838	28
3	811	839	28

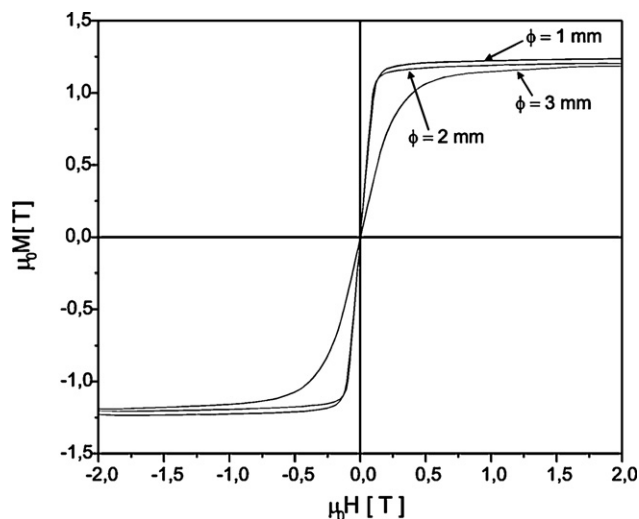


Fig. 4. Magnetic hysteresis loops of the bulk amorphous and partially crystallized  $\text{Fe}_{36}\text{Co}_{36}\text{B}_{19}\text{Si}_5\text{Nb}_4$  rods.

Table 3

Magnetic properties of the bulk amorphous and partially crystallized  $\text{Fe}_{36}\text{Co}_{36}\text{B}_{19}\text{Si}_5\text{Nb}_4$  rods.

Diameter, mm	Magnetic properties ( $M_s$ ), T	$H_c$ , A/m	$\Delta\mu/\mu$ , %
1	1.24	20.7	5.2
2	1.21	55.7	3.0
3	1.18	79.6	1.7

The saturation induction ( $M_s$ ) of the studied glassy rods has the value of 1.24 T, 1.21 T, and 1.18 T for samples with the diameters of 1 mm, 2 mm, and 3 mm, respectively (Fig. 4).

Table 2 provides information about the thermal properties and Table 3 about the magnetic properties of the studied alloys in the form of rods.

The obtained magnetic properties (Table 3) allow to classify the studied bulk alloy in the as-cast state as soft magnetic materials.

The value of Curie temperature for  $\text{Fe}_{36}\text{Co}_{36}\text{B}_{19}\text{Si}_5\text{Nb}_4$  rods of 1 mm is equal to 719 K (Figs. 5 and 6). A similar value of  $T_c$  was obtained in [3], where the result was  $T_c = 692$  K.

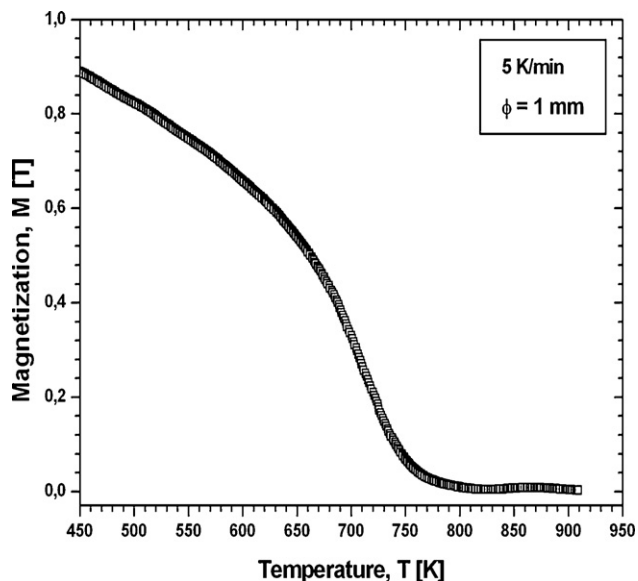


Fig. 5. Normalized magnetization versus temperature  $T$  of  $\text{Fe}_{36}\text{Co}_{36}\text{B}_{19}\text{Si}_5\text{Nb}_4$  rods with a diameter of 1 mm.

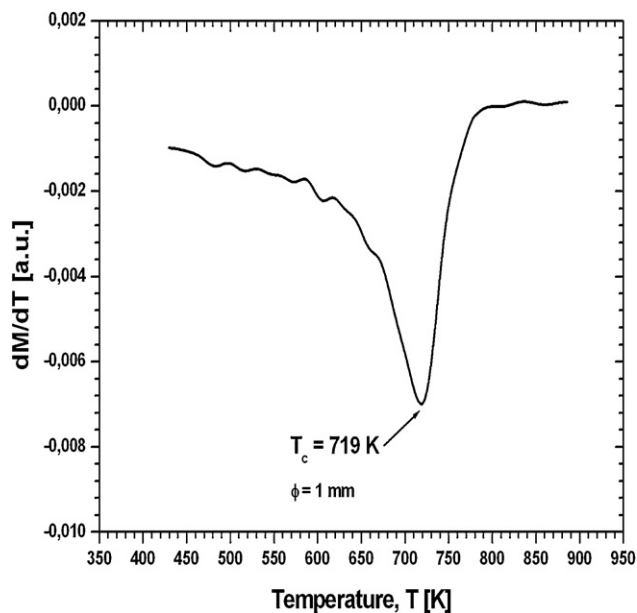


Fig. 6.  $dM/dT$  versus temperature  $T$  of  $\text{Fe}_{36}\text{Co}_{36}\text{B}_{19}\text{Si}_5\text{Nb}_4$  rods with a diameter of 1 mm.

The results obtained from Mössbauer measurements clearly shows that prolonged solidification time lead to increase in the average value of hyperfine field of amorphous matrix as well as to the formation of crystalline phase (Table 1). Increase in the value of average hyperfine field for the first amorphous phase in samples with variable diameters can be associated with decreased concentration of free volume resulting from a long solidification time [20]. The presence of additional high field components in the induction of the hyperfine field distribution, associated with the presence of nuclei or crystallites, resulted in a substantial reduction in the intensity of disaccommodation of magnetic susceptibility.

Ciurzyńska et al. showed [21] that, in nanocrystalline samples the main reason to reduce the amplitude of disaccommodation of magnetic susceptibility is the lack of directionally arranging relaxators in amorphous matrix in the sample after demagnetization. Relaxators, if present in amorphous phase, allow for change in orientation of pairs of atoms in their vicinity [20]. From this work it can also be concluded that the increase in the nanocrystalline phase content does not result in an increase in the intensity of disaccommodation amplitude, which means that the disaccommodation phenomena in this type of alloys is mainly linked to decreasing amounts of free volume in the amorphous matrix. This means that the relaxation processes occurring in the amorphous matrix are crucial for the disaccommodation of magnetic susceptibility phenomena occurring in the nanocrystalline materials based on Fe. The results obtained in this study suggest that the time of solidification of liquid alloy has an influence on the amount of structural defects and grains of the crystalline phase, which will directly affect the magnetic properties of the investigated alloys.

Rods with a diameter of 1 mm have better magnetic properties ( $H_c = 20.7$  A/m,  $\Delta\mu/\mu = 5.2\%$ , Table 3) than rods with the diameters of 2 and 3 mm ( $H_c = 55.7$  A/m and  $79.6$  A/m,  $\Delta\mu/\mu = 3\%$  and  $1.7\%$ , Table 3) of  $\text{Fe}_{36}\text{Co}_{36}\text{B}_{19}\text{Si}_5\text{Nb}_4$  alloy. These results suggest that the casting conditions influence the content of microvoids and thus also on the magnetic properties. The intensity of  $\Delta\mu/\mu$  is directly proportional to the concentration of defects in amorphous matrix, i.e. microvoids concentration [2–5]. It is obvious that value of  $H_c$  increases and value of  $\Delta\mu/\mu$  decreases with increasing of rods diameter. That results have probably corresponds with the different time of solidification, cooling rates and structures of stud-

ied samples. Moreover, values of coercivity suggest some degree of magnetic inhomogeneity (such as crystalline phase or internal stresses) in the rods. This property is very sensitive to such inhomogeneities. The detailed analysis of the magnetic properties, i.e.  $\mu_i$  and  $H_c$ , allow to classify the alloy in the as quenched state as a soft magnetic material (Table 3). These relatively good magnetic properties lead us to expect that Fe-based alloy might be used as a new engineering and functional material intended for parts of inductive components.

The content of microvoids is often examined using magnetic aftereffects ( $\Delta\mu/\mu$ ) measurements. The value of  $\Delta\mu/\mu$  increases with the increase of microvoids in the amorphous matrix [21].

The magnetic after-effects ( $\Delta\mu/\mu$ ), which are directly proportional to the microvoids concentration in the amorphous structure decrease with the increase of the diameter of the studied rods.

The value of  $H_c$  obtained for rod with a diameter of 1 mm was relatively small, but more than ten times higher, than that obtained for the same material by Shen and Inoue in [4]. For the two other samples with larger diameters, coercivity field was significantly higher. On what had surely an influence, in sample with 2 mm diameter, the presence of second amorphous phase (this phase was characterized by a large half-width of the distribution of hyperfine field, what may also suggest that there are nuclei of the crystalline phase or clusters occurring in the amorphous matrix) and in sample with largest diameter identified by Mössbauer technique  $\alpha$ -FeCo crystalline phase.

#### 4. Conclusions

The X-ray diffraction measurements and Mössbauer spectroscopy did not reveal the crystalline phase in samples in the form of rods with the diameters of 1 and 2 mm. However, for the rod with 3 mm diameter, the Mössbauer technique allow to detect a fine-crystalline phase which was identified as a  $\alpha$ -FeCo phase. The presence of this phase may be linked with prolonged solidification of liquid alloy during production process.

The investigated alloys have good soft magnetic properties. These relatively good magnetic properties lead us to expect that the investigated amorphous alloy is promising for future applications as a new engineering and functional material for the parts of force sensors and other applications. Moreover, force sensors based on newly developed amorphous and nanocrystalline alloys may operate in the high-temperature range. The temperature of operation

of such a sensor is limited mainly by the Curie temperature and the value of  $T_C$  for the  $\text{Fe}_{36}\text{Co}_{36}\text{B}_{19}\text{Si}_5\text{Nb}_4$  alloy which amounts to 719 K.

#### Acknowledgment

This work was supported by Polish Ministry of Science (grant N507 027 31/0661).

#### References

- [1] A. Inoue, Materials Transactions JIM 36 (7) (1995) 866–875.
- [2] M.E. McHenry, M.A. Willard, D.E. Laughlin, Progress in Materials Science 44 (1999) 291–433.
- [3] A. Inoue, B.L. Shen, C.T. Chang, Intermetallics 14 (2006) 936–944.
- [4] B. Shen, A. Inoue, Applied Physics Letters 85 (21) (2004) 4911–4913.
- [5] R. Nowosielski, R. Babilas, Journal of Achievements in Materials and Manufacturing Engineering 20 (2007) 487–490.
- [6] M. Nabałek, J. Zbrozarczyk, J. Olszewski, M. Hasiak, W. Cieurzyńska, K. Sobczyk, J. Świerczek, J. Kaleta, A. Łukiewska, Journal of Magnetism and Magnetic Materials 320 (2008) 787–791.
- [7] P. Vojtanik, Journal of Magnetism and Magnetic Materials 304 (2006) 159–163.
- [8] A. Inoue, B. Shen, A. Takeuchi, Materials Science and Engineering A441 (2006) 18–25.
- [9] R. Nowosielski, R. Babilas, G. Dercz, L. Pająk, Solid State Phenomena 163 (2010) 165–168.
- [10] G. Badura, J. Rasek, Z. Stokłosa, P. Kwapuliński, G. Haneczok, J. Lelątko, L. Pająk, Journal of Alloys and Compounds 436 (2007) 43–50.
- [11] P. Kwapuliński, Z. Stokłosa, J. Rasek, G. Badura, G. Haneczok, L. Pająk, L. Lelątko, Journal of Magnetism and Magnetic Materials 320 (2008) 778–782.
- [12] Z. Stokłosa, J. Rasek, P. Kwapuliński, G. Haneczok, G. Badura, J. Lelątko, Materials Science and Engineering C 23 (2003) 49–53.
- [13] P. Kwapuliński, J. Rasek, Z. Stokłosa, G. Haneczok, Journal of Magnetism and Magnetic Materials 254–255 (2003) 413–415.
- [14] Ł. Madej, L. Bednarska, V. Nosenko, B. Kotur, A. Chrobak, G. Haneczok, Chemistry of Metals and Alloys 1 (2008) 333–337.
- [15] D. Szewiczek, S. Lesz, Journal of Materials Processing Technology 157–158 (2004) 771–775.
- [16] D. Szewiczek, S. Lesz, Journal of Materials Processing Technology 162–163 (2005) 254–259.
- [17] J. Frąckowiak (ed.), University of Silesia, Scientific Papers of the University of Silesia (1993) (In Polish).
- [18] M. Stoica, R. Li, A. Reza, Yavari, G. Vaughan, J. Eckert, N. Van Steenberge, D. Ruiz Romera, 504S (2010) S123–S128.
- [19] B. Wunderlich, Macromolecular Physics, vol. 2 Crystal Nucleation, Growth, Annealing, Academic Press Inc., New York, San Francisco, London, 1976.
- [20] J. Zbrozarczyk, L.K. Varga, J. Olszewski, W. Cieurzyńska, B. Wysłocki, S. Szymura, M. Hasiak, G. Haneczok, Journal of Magnetism and Magnetic Materials 160 (1996) 279–280.
- [21] W.H. Cieurzyńska, Physics Sery 2, Częstochowa (2002) Poland, ISBN 83-87745-41-3 (In Polish).